The Self-Equalizing De Bruijn Sequence for 3D Profilometry

Tomislav Petković
tomislav.petkovic.jr@fer.hr
Tomislav Pribanić
tomislav.pribanic@fer.hr
Matea Đonlić
matea.donlic@fer.hr

University of Zagreb
Faculty of Electrical Engineering and Computing
Unska 3, HR-10000 Zagreb, Croatia

Abstract

Using color in 3D profilometry usually requires a tedious color calibration to mitigate the undesired effects of ambient lighting, object albedo, non-equal channel gains, and channel cross-talk. We propose a novel De Bruijn sequence for multi-channel structured light that removes the need for color calibration of a camera-projector pair. The proposed sequence has the following desirable properties: (1) it enables the extraction of ambient lighting, (2) it enables the cancellation of object albedo, and (3) it enables the equalization of channel gains.

1 Introduction

Three-dimensional non-invasive surface profilometry using structured light is a widely studied topic in the field of computer vision with applications ranging from industrial inspection to human-computer interaction. Almost all current approaches use a digital projector to project a structured light pattern and a digital camera to record it. One of the most important issues of all such system is the design of the structured light pattern: the pattern must enable reconstruction robust to the ambient light and to the characteristics of the observed object.

Structured light patterns may be classified in various ways [10]. The simplest classification distinguishes *one-shot* patterns that enable reconstruction from a single image and *multi-shot* patterns that require more than one image. There is usually a resolution/time trade-off involved: one-shot patterns yield a sparser reconstruction than multi-shot ones, but have a shorter acquisition time. Today a well-designed pattern should enable both one- and multi-shot reconstruction. Such patterns were proposed by Li Zhang et al. [13] for color light and Yueyi Zhang et al. [14] for monochromatic light.

In this work we focus on color structured light. Color structured light patterns described in the literature include fringe patterns [12], colored grids [9], N-ary color codings [1], and De Bruijn sequences [6, 13, 16]. The most important work by Caspi et al. [1] describes the color imaging model that captures all the major problems of using color: ambient lighting, object albedo, non-equal channel gains, and channel cross-talk. Almost all of these problems are mitigated via the color calibration procedure, e.g. of Caspi et al. [1] or of Juang and

Majumder [5], that must be performed prior to every imaging to include the object albedo. If calibration is performed once then the object albedo is removed by an adaptive channel equalization scheme [16] or by an adaptive color fitting [2], however, such approaches require either object segmentation or assumption of a constant albedo in the scene.

In this article we propose a novel De Bruijn sequence for color (or multi-channel) structured light which we call the *self-equalizing* sequence. The sequence has several desirable properties: (1) it enables the extraction of ambient lighting, (2) it enables the cancellation of object albedo, and (3) it enables the equalization of channel gains. The proposed sequence thus effectively removes the need for a precise color calibration of the imaging system, requiring only geometric calibration. Additionally, the proposed sequence enables a dense multi-shot reconstruction for static objects and a sparse one-shot reconstruction for moving objects. To the best of our knowledge none of the previous works attempted to design such a pattern. Most of the previous works use a non-altered De Bruijn sequence or impose a simple additional constraint on adjacent colors only. Our approach defines a novel constraint on the entire De Bruijn window in such way to achieve the aforementioned properties. The proposed sequence shares one characteristic with the sequence of [3]: it has the same V channel, but is otherwise different.

2 Structured Light Pattern

We propose a novel cyclic color structured light pattern of which *any frame* may be used for one-shot reconstruction and of which *any consecutive m* frames may be used for multi-shot reconstruction. The pattern is based on a generalized De Bruijn sequence on which we impose additional constraints that enable the robust estimation of the projected color.

2.1 Self-Equalizing De Bruijn Sequence

A k-ary De Bruijn sequence of order n is a cyclic sequence of length $L = k^n$ over an alphabet of k symbols in which every subsequence of length n, called a window, appears exactly once on the cycle [8]. A De Bruijn sequence is associated with Eulerian cycle of a De Bruijn digraph which may be used to generate it. The De Bruijn digraph contains k^{n-1} vertexes and k^n directed edges, where an outgoing edge labeled d_e (here d is a symbol from the alphabet) connects a vertex labeled $d_1 d_2 \cdots d_{n-1}$ to a vertex $d_2 \cdots d_{n-1} d_e$, therefore concatenating vertex and edge labels yields a window $W = d_1 d_2 \cdots d_l \cdots d_{n-1} d_e$ of length n.

Let c be the number of channels. A full De Bruijn digraph is constructed over an alphabet of $k = 2^c - 2$ symbols. Every symbol d is represented by a c-digit binary number where value of jth digit indicates if jth channel is on (1) or off (0). Note we disallow black and white where all digits of d are the same. We propose the following two constraints that every De Bruijn window W of length n must satisfy: (a) the jth digit should attain value 0 for at least one d_l in W and (b) the jth digit should attain value 1 for at least one d_l in W. These constraints ensure that all channels span the full available dynamic range, and are sufficient for the robust estimation of the projected color (see Section 3). We call a De Bruijn sequence satisfying the two constraints *self-equalizing*. The proposed sequence is constructed as Eulerian cycle in the pruned De Bruijn graph where edges belonging to the invalid windows are removed.

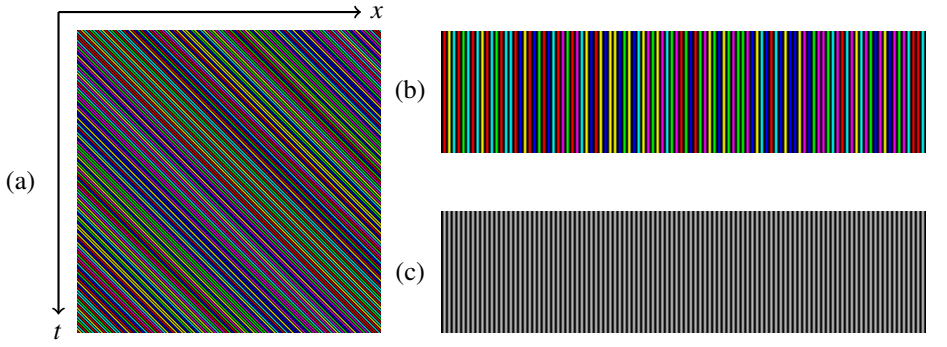

Figure 1: Structured light pattern for $c = 3$, $k = 6$, and $n = 3$ that contains $L = 102$ stripes. (a) shows how the pattern defined by Eq. (1) changes over x and t. (b) shows the first image in the sequence for $t = 0$; it is the first row in (a). (c) is the V channel of (b).

2.2 Cyclic Sequence of Images

The full length light pattern is a cyclic sequence of images whose cycle is comprised of $L \cdot S$ frames, of which any one frame is sufficient for one-shot reconstruction, and of which any $m = n \cdot S$ consecutive frames are sufficient for multi-shot reconstruction. $S \geq 3$ is the number of phase shifts per symbol. Let $d_1 d_2 \cdots d_L$ be a sequence satisfying the aforementioned constraints. The intensity of the ith channel of the frame at time $t \in \mathbb{Z}$ is

$$I(x,t,i) = I_{i,\max} \sum_{l=0}^{L-1} \mathbf{1}_i(d_{l+1}) \Big(\frac{1}{2} - \frac{1}{2} \cos\big(2\pi \frac{x - lP}{P} - \varphi_t\big) \Big) \operatorname{rect}\Big(\frac{\tilde{x}}{P} - \frac{1}{2} \Big), \tag{1}$$

where x is the image column index (image width must be greater than $L \cdot P$, all rows are the same), P is the period of the fringe, $\varphi_t = 2\pi t / S$ is the phase shift, and $I_{i,\max}$ is the maximal channel intensity. The variable $\tilde{x} = x - lP - \varphi_t \frac{P}{2\pi} \mod L \cdot P$ ensures the rectangular function is periodically extended. The function $\mathbf{1}_i$ is the indicator function of ith channel, i.e. $\mathbf{1}_i(d_l) = 1$ if d_l contains the channel i and 0 otherwise.

We give an example for the RGB color-space ($c = 3$, $k = 2^c - 2 = 6$) where the symbols of the alphabet are: red (R), green (G), yellow (Y), blue (B), magenta (M), and cyan (C). Of full 216 digraph edges after pruning using the proposed constraints exactly 102 digraph edges remain. One possible sequence of 102 symbols is RYCRGCRCYRCGRCCRBYRBGRBCRMG-RMCYBRYBYYBGYBCYMGYMCGMRGBRGMYGBYGMGGMBYCBRCBYBBYMBGMMGCMRCMY-CMGBMYBMGMCRRC for which the pattern is shown in Fig. 1. Note that: (a) the V channel (the maximum of all channels) is a harmonic function enabling application of phase shifting, (b) all channels are coherent in phase which supports the spatial analysis, and (c) the full-length pattern is cyclic and repeats after $L \cdot S$ frames without any discontinuities.

3 Channel Equalization

When using color structured light the projected color must be correctly identified from the data recorded by the camera. A compensation scheme for ambient lighting, object's albedo, channel gains, and channel cross-talk is necessary. It is usually achieved by applying an

imaging model whose parameters are obtained during color calibration. One model for RGB color-space widely accepted in the literature is proposed by Caspi et al. [1]:

$$\underbrace{\begin{bmatrix} R \\ G \\ B \end{bmatrix}}_{I_c} = \underbrace{\begin{bmatrix} a_{RR} & a_{RG} & a_{RB} \\ a_{GR} & a_{GG} & a_{GB} \\ a_{BR} & a_{BG} & a_{BB} \end{bmatrix}}_{A} \underbrace{\begin{bmatrix} k_R & 0 & 0 \\ 0 & k_G & 0 \\ 0 & 0 & k_B \end{bmatrix}}_{K} f\Big(\underbrace{\begin{bmatrix} r \\ g \\ b \end{bmatrix}}_{I_p} \Big) + \underbrace{\begin{bmatrix} R_0 \\ G_0 \\ B_0 \end{bmatrix}}_{I_0}, \tag{2}$$

where I_c is the color recorded by the camera, A is the channel transfer matrix, K is the albedo matrix, f is a monotonic function modeling projector's non-linearity, I_p is the color instruction to the projector, and I_0 is the ambient lighting. We propose a simplified model where ith channel is modeled as

$$I_c(i) = h(i)I_p(i) + I_0(i), \tag{3}$$

i.e. the projector non-linearity f is disregarded and matrices A and K are combined into one diagonal matrix whose elements are represented via coefficient h, so the channel cross-talk is disregarded. Note that for the RGB color-space $h(1) = a_{RR}k_R$ etc. The cross-talk may be omitted if the color filters of the projector and the camera are well matched, which holds for standardized consumer electronics and which was also noted by Caspi et al. [1]. In Section 5.2 we discuss how disregarding the non-linearity does not affect spatial nor temporal processing of the proposed pattern.

Combining the model (3) with the constraints imposed on the De Bruijn sequence allows the recovery of $I_p(i)$ from $I_c(i)$ independently for each channel. The projected value is recoverable as $I_p(i) = \big(I_c(i) - I_0(i)\big)/h(i)$, where $I_0(i)$ and $h(i)$ are estimated from the recorded frame(s) using either spatial or temporal analysis.

For the spatial analysis only one frame is used. Parameters $I_0(i)$ and $h(i)$ are recovered by considering n spatially adjacent stripes that form one window W. Let $m(i)$ be the minimal and let $M(i)$ be the maximal value per channel at the peak positions of n adjacent stripes. Under the assumption of spatial invariance ($I_0(i)$ and $h(i)$ are the same for n adjacent stripes) we have $I_0(i) = m(i)$ and $h(i) = M(i) - m(i)$ as W satisfies the imposed constraints. The procedure is illustrated in Fig. 2 for the RGB color-space and $n = 3$: a scanline orthogonal to the stripe direction is used to identify $n-1$ stripes adjacent to the central stripe. Channel values are then extracted along the scanline at stripe peaks.

The temporal analysis is performed for every pixel independently. Parameters $I_0(i)$ and $h(i)$ are recovered by considering $n \cdot S$ consecutive frames that span one window W. Again, let $m(i)$ be the minimal and let $M(i)$ be the maximal value per channel. Under the assumption of temporal invariance (static scene) we have $I_0(i) = m(i)$ and $h(i) = M(i) - m(i)$ as W satisfies the imposed constraints.

Therefore, both spatial and temporal analysis enable simple channel equalization that effectively removes undesired influence of ambient lighting, object's albedo, and unequal channel gains.

4 3D Reconstruction

As stated before *any frame* from the proposed structured light sequence may be used for the one-shot reconstruction and *any consecutive* $m = n \cdot S$ frames may be used for the multi-shot reconstruction. In this section we describe how to identify the projector light plane; once the light plane is identified the reconstruction uses the standard triangulation principle.

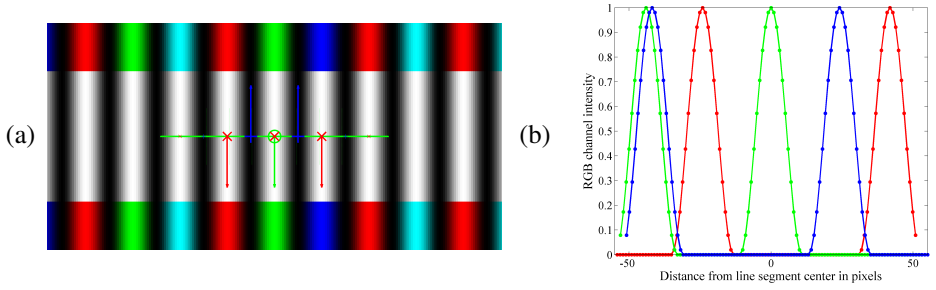

Figure 2: Example of spatial channel equalization for $n = 3$ and RGB color-space. (a) shows spatial position of the scanline orthogonal to the central stripe; the central part is shown in gray-scale for visualization purposes and sample points are marked with x. (b) shows channel values along the scanline.

4.1 One-Shot Spatial Reconstruction

Single-shot spatial reconstruction is performed for every frame independently in the following steps: (a) a modified multi-scale vesselness is computed; (b) the positions of color stripes and of black slits are extracted; (c) scanlines are placed orthogonally to every detected stripe and $n-1$ adjacent stripes are extracted; (d) only n-tuples that satisfy a *spatial invariance condition* are retained; (e) channels are equalized as described in Section 3, but only for the n-tuples identified in (d); and (f) stripe positions are decoded using the window property.

The multi-scale vesselness map $\mathcal{V}$ is introduced by Frangi et al. [9]. We use a modified vesselness that extracts both bright (color stripes, $\mathcal{V} > 0$) and dark (black slits, $\mathcal{V} < 0$) ridges:

$$\mathcal{V} = \operatorname{sign}(-\lambda_{1,\sigma}) \max_{\sigma_{\min}<\sigma<\sigma_{\max}} \left\{ \exp\left(-\alpha \left| \frac{\lambda_{2,\sigma}}{\lambda_{1,\sigma}} \right|\right) \left(1 - \exp\left(-\beta(\lambda_{1,\sigma}^2 + \lambda_{2,\sigma}^2)\right)\right) \right\}, \qquad (4)$$

where $\lambda_{1,\sigma}$ and $\lambda_{2,\sigma}$, $|\lambda_{1,\sigma}| > |\lambda_{2,\sigma}|$, are eigenvalues of the Hessian matrix at scale σ and where $\alpha, \beta \in \mathbb{R}^+$ are constants. Color stripes are found as the local maxima in $\mathcal{V}$ and black slits are found as the local minima of (4). The sub-pixel positions are then determined as described in [11].

The vesselness map is computed using the average of all channels as input. The proposed pattern of Eq. (1) is spatially coherent as all channels are modulated by the same harmonic function; adding them together improves the visibility of stripes even prior to channel equalization. Using the V channel instead the average may reduce the performance as spatial equalization cannot be performed before stripes are found. Note that unlike previous works that use either horizontal or vertical scanlines we use a true 2D analysis. This is necessary as spatial equalization requires adjacent stripes in the direction orthogonal to the central stripe of the window; the eigenvector of the Hessian associated with λ_1 gives the required direction (see [11]).

Once the scanline is placed orthogonally to the color stripe (see Fig. 2) the closest adjacent $n-1$ stripes are identified. We define the *spatial invariance condition* as one where the extracted n-tuple fulfills the following: (a) the distances between adjacent stripes are $\sim 4\sqrt{3}(\sigma - 0.5)$ px, where σ is the scale of (4), (b) the color stripe directions are parallel, and (c) there is exactly one black slit between every two adjacent stripes.

No.	1	2	3	4	5	6	7	8	9
Red	576	650	400	600	800	400	500	800	800
Blue	640	600	400	600	800	600	800	700	500
$\mu\,[^\circ]$	-1.0	-1.1	-1.0	-1.1	-1.3	-0.5	-0.6	-1.5	-1.9
$\sigma\,[^\circ]$	5.9	6.2	7.6	6.0	7.0	6.0	6.3	6.7	7.8

Table 1: Circular mean and circular deviation (in degrees) of the difference in wrapped phases for various channel gains. Measurement 1 uses auto white balance gains, measurement 2 uses true white balance gains (SpyderCUBE$^{\text{TM}}$calibration), and measurements 3-9 use several manually chosen gains.

Finally, the colors are identified using a simple thresholding with the threshold set at half-value of the dynamic range of every equalized channel. Every color n-tuple then, due to the window property, directly identifies one projector light plane.

4.2 Multi-Shot Temporal Reconstruction

Multi-shot temporal reconstruction is performed for every pixel independently in the following steps: (a) channels are equalized as described in Section 3; (b) the wrapped phase is computed from the equalized V channel; (c) stripes are detected using the window uniqueness property; and (d) the wrapped phase is unwrapped.

The following analysis assumes static (temporally invariant) scene. The wrapped phase is computed from any consecutive $n \cdot S$ frames starting from the frame at reference time t_0 as

$$\psi_w = \operatorname{atan2}\Big(-\sum_{t=t_0}^{t_0+n\cdot S} V_{\text{eq}}(t)\sin(\varphi_t), \sum_{t=t_0}^{t_0+n\cdot S} V_{\text{eq}}(t)\cos(\varphi_t)\Big), \tag{5}$$

where $V_{\text{eq}}(t)$ is the equalized V channel at time t. The phase ψ_w corresponds to the temporal intensity model $V_{\text{eq}}(t) = V_0 + V_1\cos(\psi_w + \varphi_t)$ of the equalized V channel which achieves its maxima at $\psi_w + \varphi_t = 2k\pi$, $k \in \mathbb{Z}$. As $\varphi_t = 2\pi t/S$ the maxima occur at time steps $t_{\max}(k) = t_0 - \frac{1}{2\pi}\psi_w S + kS$, $k \in \mathbb{Z}$. Decoding De Bruijn symbols for $t_{\max}(k)$ that fall into $[t_0, t_0 + n\cdot S]$ interval yields a time-reversed window $W_R = d_n d_{n-1}\cdots d_1$ from which the phase unwrapping offset is computed. As $\psi_w \in \langle -\pi, \pi]$ either values $k = 0, 1, \ldots n-1$ or $k = 1, 2, \ldots, n$ produce the required $t_{\max}(k) \in [t_0, t_0 + n\cdot S]$. The former solution gives the position of $W = d_1 d_2 \cdots d_n$ directly for the reference time step t_0, e.g. if W is at position j then the unwrapped phase is $\psi_u = -\psi_w + 2\pi j$. The latter solution requires an additional phase shift of 2π as we are decoding the adjacent window, so $\psi_u = -\psi_w + 2\pi(j+1)$. This additional phase shift is caused by the discontinuity of the atan2 function, but, as we use ψ_w directly, the discontinuity elegantly translates into one additional shift only for those pixels that require it. Also note that the obtained times $t_{\max}(k)$ are not in $\mathbb{Z}$ so we linearly interpolate between two closest time steps t.

5 Results and Discussion

All presented experiments were performed using Acer X1260 DLP projector, PointGrey DragonFly2 DR-HICOL camera, and Fujinon HF9-HA1B lens. The resolution of both projector and camera is 1024×768. The camera-projector distance was ~ 11 cm. The working distance was ~ 1 m. The calibration volume was $\sim 0.5 \times 0.5 \times 0.5$ m. A geometric calibration

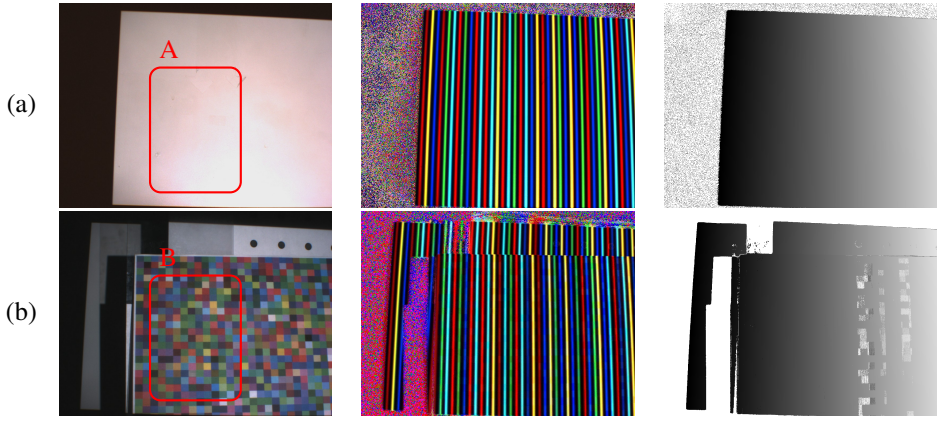

Figure 3: A white planar surface (a) and a planar color checkerboard (b). The first column shows camera FOV with two ROIs, the second column shows first equalized image of $n \cdot S$ images, and the third column shows the unwrapped phase of the multi-shot method.

of the camera and the projector was performed as described in [15]. The camera has a Bayer pattern that effectively reduces the spatial resolution making the sequence of Section 2.2 unusable due to too narrow stripes. Therefore, for the experiments we generated a shorter sequence RYBRGCRGBRCRCYRCGRCBYRBYGBYBGRBGYBCRBCYBYCBRYC ($n = 3$, $P = 22$, and $S = 4$) that produces wider stripes.

We have performed three experiments: (1) the influence of channel gains, (2) the reconstruction of white and colored planar surfaces, and (3) qualitative reconstructions of several objects: fruits and vegetables, a human face, and a human hand.

5.1 Experiments

For the first experiment we tested the influence of channel gains to phase estimation of the multi-shot method. The camera allows setting the red and blue channel gains according to IIDC v1.32 specification [7] while the green gain is fixed. We compared the wrapped phase of the proposed method and of the traditional gray-level fringe shifting for several noticeably off-balance channel gains and for the balanced gains. The imaged objects were fruits and vegetables shown in the first column in Fig. 4 (default channel gains), so the scene contained several different albedos. The table 1 lists circular means and circular deviations in degrees for 9 different gain pairs. Note that the mean is always close to zero and that the variance is always less than 8° (which is about one projector pixel for the center of the working area). Overall, the *self-equalization* property effectively cancels the influence of varying channel gains and of different albedos.

For the second experiment we reconstructed two planar surfaces shown in Fig. 3: a white surface and a challenging random color checkerboard. Note the perfect reconstruction for the whole white surface and for the ROI B of the checkerboard pattern. Artifacts on the right side of the checkerboard pattern were caused by the channel cross-talk that is not accounted for in the proposed model, in this case specifically from green to blue channel. Note that such artifacts are not expected for normal objects and that including the cross-talk would eliminate them. The residual error of the fitted 3D plane for the marked ROIs is 0.7463 ± 0.5483 mm

for A and 0.7802 ± 0.5682 mm for B.

For the third experiment both projector and camera were used with the default factory settings simulating the most common usage scenario. The three imaged objects and the processing steps are shown in Fig. 4 where: (a) is the first of $n \cdot S$ images; (b) is temporally equalized (a); (c) is the wrapped phase computed using Eq. (5); (d) is the unwrapped phase; (e) is spatially equalized (a); (f) is textured 3D reconstruction using multi-shot method of Section 4.2; and (g) is textured 3D reconstruction using one-shot method of Section 4.1 using only image (a). Note that both temporal and spatial equalization successfully remove the ambient lightning, object albedo, and varying channel gains.

5.2 Discussion

The performed experiments demonstrate the *self-equalization* property of the proposed pattern and showcase both one- and multi-shot 3D reconstruction from the same data. The one-shot reconstruction is spatially sparser and requires the imaged object to be sufficiently wide, e.g. for the hand image in Fig. 4 the thumb and the forefinger are partially reconstructed while the remaining fingers are lost as they are too narrow. Generally, the proposed spatial scheme is applicable only if the object is wider than $n \cdot P$ projector pixels. This is equivalent to requirement for the multi-shot method: the object must not move during any consecutive $n \cdot S$ frames. Similar constraints exists for all one-shot methods; using a projector-camera pair with a better spatial resolution enables imaging of narrower objects.

The one-shot method provided already satisfactory results even though the decoding step has been carried out directly, i.e. an additional processing step such as the dynamic programming of [13] would further improve the results. The pattern is also compatible with the one of [3] making a dense one-shot reconstruction an option, with a possible improvement if the windowed Fourier transform is applied to the scanlines of Section 4.1 that give the optimal window orientation and width.

The omitted projector non-linearity $f(\cdot)$ does not affect the spatial and temporal processing: $f(\cdot)$ is monotonic so the maxima and minima of the pattern always remain at same spatial position, only the perceived stripe width may change. Therefore, the spatial processing returns the true stripe centers. Phase estimation is similarly not affected as the phase of $f\big(\cos(\cdot)\big)$ and $\cos(\cdot)$ is almost the same. Furthermore, the pattern is coherent in all channels which improves the spatial detection and does not affect the phase estimation. However, the coherence may increase channel cross-talk effects as the maxima of channels coincide; note that this only affects the color decoding step.

Most of the consumer grade cameras use Bayer sensors so the limiting factor for the stripe width is usually the camera and not the projector: the crest of every stripe should not be narrower than the size of the 3×3 Bayer grid. Note that the proposed method is especially suitable if a high-speed monochrome camera is paired with a DLP projector as the same color wheel having minimal or no cross-talk may be used for both.

Compared to other De Bruijn based patterns described in the literature we chose a harmonic modulating function to avoid problems with striped patterns where edges are the detected features: due to blooming effects the edge between stripes of differing brightness will move while the position of the ridge will remain unaffected.

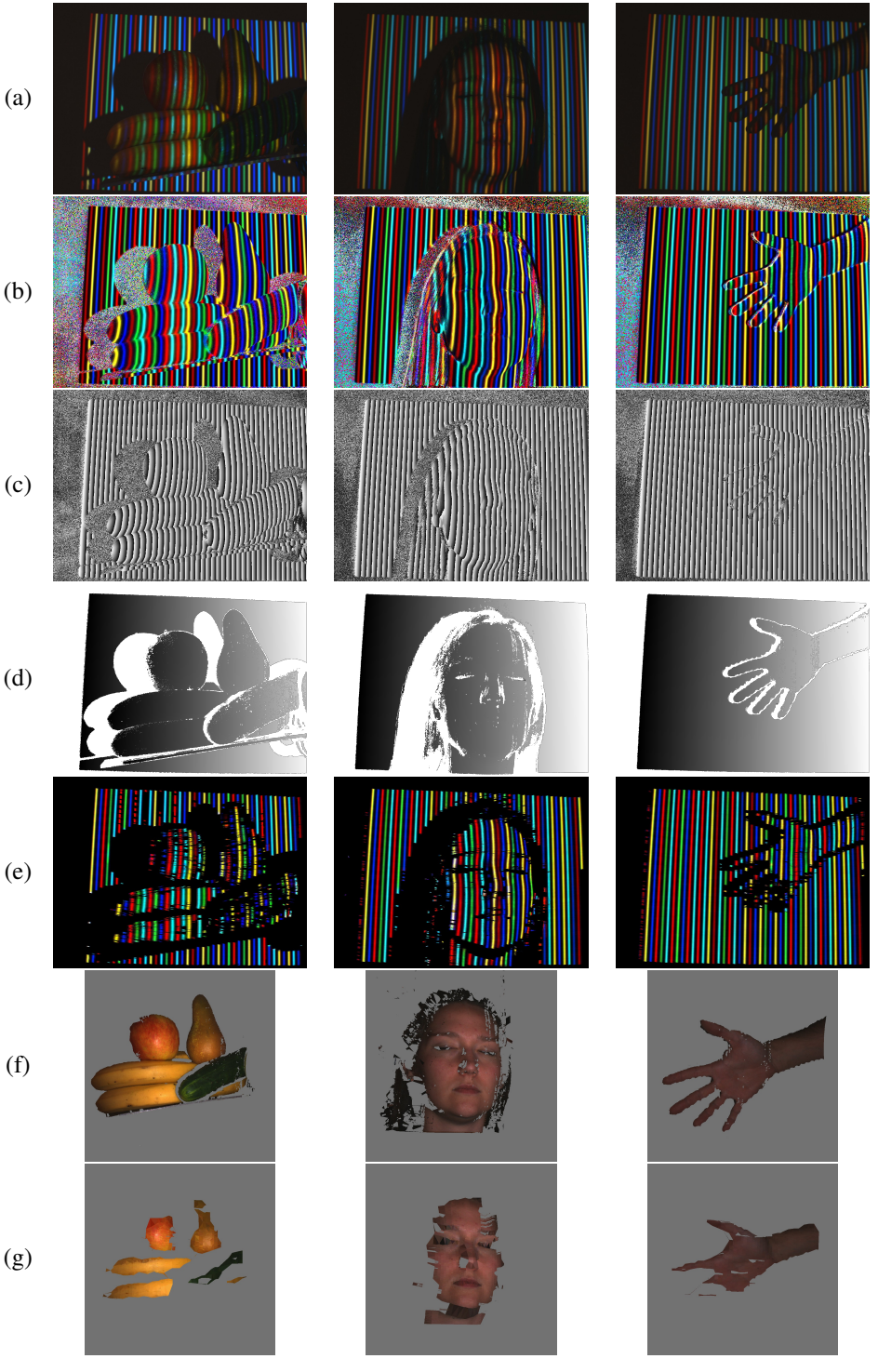

Figure 4: Example reconstructions for three scenes: fruits and vegetables, a face, and a hand.

6 Conclusion

We have proposed the *self-equalizing* De Bruijn sequence that enables time-continuous 3D profilometry where any single frame from the sequence may be used for one-shot reconstruction and where any consecutive $m = n \cdot S$ frames may be used for multi-shot reconstruction.

We have theoretically explained and experimentally demonstrated the following desirable properties of the proposed *self-equalizing* sequence: (1) the removal of ambient lighting, (2) the removal of object albedo, and (3) the equalization of channel gains.

Future work will focus on including the channel cross-talk in two ways, through a color calibration step under the assumption of constant cross-talk coefficients, and through an additional constraint on the sequence that enables on-line recovery of all parameters of Eq. (2). Additionally, we plan to implement a movement detection in an approach similar to [14].

Acknowledegements

This work has been fully supported by Croatian Science Foundation under Project No. IP-11-2013-3717. We are grateful to Professor Joaquim Salvi whose suggestions improved the content and the presentation of this paper.

References

[1] Dalit Caspi, Nahum Kiryati, and Joseph Shamir. Range imaging with adaptive color structured light. *Pattern Analysis and Machine Intelligence, IEEE Transactions on*, 20 (5):470–480, May 1998. ISSN 0162-8828. doi: 10.1109/34.682177.

[2] Philipp Fechteler and Peter Eisert. Adaptive color classification for structured light systems. In *Computer Vision and Pattern Recognition Workshops, 2008. CVPRW '08. IEEE Computer Society Conference on*, pages 1–7, June 2008. doi: 10.1109/CVPRW.2008.4563048.

[3] Sergio Fernandez and Joaquim Salvi. One-shot absolute pattern for dense reconstruction using De Bruijn coding and windowed fourier transform. *Optics Communications*, 291(0):70–78, 2013. ISSN 0030-4018. doi: 10.1016/j.optcom.2012.10.042.

[4] Alejandro F. Frangi, Wiro J. Niessen, Koen L. Vincken, and Max A. Viergever. Multiscale vessel enhancement filtering. In William M. Wells, Alan Colchester, and Scott Delp, editors, *Medical Image Computing and Computer-Assisted Intervention MICCAI'98*, volume 1496 of *Lecture Notes in Computer Science*, pages 130–137. Springer Berlin Heidelberg, 1998. ISBN 978-3-540-65136-9. doi: 10.1007/BFb0056195.

[5] Ray Juang and Aditi Majumder. Photometric self-calibration of a projector-camera system. In *Computer Vision and Pattern Recognition, 2007. CVPR '07. IEEE Conference on*, pages 1–8, June 2007. doi: 10.1109/CVPR.2007.383468.

[6] Jordi Pagès, Joaquim Salvi, Christophe Collewet, and Josep Forest. Optimised De Bruijn patterns for one-shot shape acquisition. *Image and Vision Computing*, 23(8): 707–720, 2005. ISSN 0262-8856. doi: 10.1016/j.imavis.2005.05.007.

[7] *Register Reference for Point Grey Digital Cameras*. Point Grey, 3.1 edition, June 2013. URL https://www.ptgrey.com/support/downloads/10130/.

[8] Frank Ruskey. *Combinatorial generation*. University of Victoria, Victoria, preliminary working draft edition, 2003.

[9] J. Salvi, J. Batlle, and E. Mouaddib. A robust-coded pattern projection for dynamic 3D scene measurement. *Pattern Recognition Letters*, 19(11):1055–1065, 1998. ISSN 0167-8655. doi: 10.1016/S0167-8655(98)00085-3.

[10] Joaquim Salvi, Sergio Fernandez, Tomislav Pribanić, and Xavier Lladó. A state of the art in structured light patterns for surface profilometry. *Pattern Recognition*, 43(8): 2666–2680, 2010. doi: 10.1016/j.patcog.2010.03.004.

[11] Carsten Steger. An unbiased detector of curvilinear structures. *Pattern Analysis and Machine Intelligence, IEEE Transactions on*, 20(2):113–125, Feb 1998. ISSN 0162-8828. doi: 10.1109/34.659930.

[12] Clarence Wust and David W. Capson. Surface profile measurement using color fringe projection. *Machine Vision and Applications*, 4(3):193–203, 1991. ISSN 0932-8092. doi: 10.1007/BF01230201.

[13] Li Zhang, Brian Curless, and Steven M. Seitz. Rapid shape acquisition using color structured light and multi-pass dynamic programming. In *3D Data Processing Visualization and Transmission*, pages 24–37, 2002. doi: 10.1109/TDPVT.2002.1024035.

[14] Yueyi Zhang, Zhiwei Xiong, Zhe Yang, and Feng Wu. Real-time scalable depth sensing with hybrid structured light illumination. *Image Processing, IEEE Transactions on*, 23 (1):97–109, Jan 2014. ISSN 1057-7149. doi: 10.1109/TIP.2013.2286901.

[15] Zhengyou Zhang. A flexible new technique for camera calibration. *Pattern Analysis and Machine Intelligence, IEEE Transactions on*, 22(11):1330–1334, Nov 2000. ISSN 0162-8828. doi: 10.1109/34.888718.

[16] Yu Zhou, Dongwei Zhao, Yao Yu, Jie Yuan, and Sidan Du. Adaptive color calibration based one-shot structured light system. *Sensors*, 12(8):10947–10963, 2012. doi: 10.3390/s120810947.